AMSE JOURNALS-AMSE IIETA publication-2017-Series: Modelling C; Vol. 78; N°4; pp 478-495

Submitted Feb. 2017; Revised March 15, 2017, Accepted April 15, 2017

https://doi.org/10.18280/mmc_c.780406

Research and Application of Mineral Deposit Modeling Technology

Jun Liu

Qigihar Mineral Exploration and Development Institute of Heilongjiang Province, Jianhua District, Qigihar, China, 161006 (Guida65@163.com)

Abstract

This paper describes the contour veneer method, from the angle of rebuilding of contour appearance, turning it into the issue to seek the most advantage way in the loop diagram. Because of its disadvantage in operational speed, it is proposed to use multi resolution veneer processing and to reduce the contour distinguishing efficiency with wavelet differentiation. When the discrimination efficiency is low, the operation way of contour veneer would be used, then add vertexes one by one into the present appearance and make the appearance generate new changes. At the same time, the paper discusses the construction method of the transition external lines based on the way of the central axis, and carries out the cross treatment on the branch problem. Taking a deposit as the reference, create the surface appearance model of fracture surface and surface model of mineral geological body and conduct anti Delaunay triangulation subdivision to realize the combination of geological body as well as engineering model and tetrahedron mesh model. The obtained model could accurately calculate the numerical value of rock mining project in complex geological environment.

Key words

Digital mine, 3D model of mineral deposit, tiling Algorithm, branch treatment.

1. Introduction

Digital mine software system takes three-dimensional geological modeling of deposit as the foundation and focus and conduct simulation reconstruction of three-dimensional geological scene of deposit, including the modeling of ground level, fault level and mineral geological body and the speculation of geological attribute variables[1]. By using mining geological situation in three-dimensional form, real data could be provided to support the exploration and study mining geological variables including space change, mining creation, resource control, production objectives setting etc. Australia and the United States are more advanced in the development of mining industry, and the mineral three-dimensiona geological model softwares that they establish are very popular in the world. In our country, some research institutes and related agencies have also made the purchase of the software and conduct constant study and development of them in the practical application. However, there are certain shortages in the use of such softwares in our country, and the cost is very expensive. Although our country has taken part in this area and realized some creations, but because economic support is not enough, the difficulty coefficient of the creation is very high, so our technology is far behind the European and American countries [2]. The associated operation methods and science technologies are of far-reaching significance, especially in the research and development of some commercial software. Through market competition and survival of the fittest to accelerate the development of its mature, and the digital mine construction of the timeliness will be improved.

In this paper, the current three-dimensional numerical modeling is analyzed, and the exterior line tiling method based on the reconstruction of exterior line and surface is described and the improved. Analysis of the improved external line tiling algorithm is focused on.

2. Borehole data visualization technology

The original sources of geological related data varies, and the numerical value of drilling engineering is the most typical, other numerical value could also be converted into drilling value, but it needs to conduct an operation[3].

2.1 Space trajectory calculation

The process of drilling holes will be interfered by the trend of rock layer, drilling direction, hardness of the rock and rock hardness. The trail of drilling holes can be seen as a complex and

continuous arc, which is shown specifically in figure 1. In geological detection, drilling trace mathematical modeling methods commonly used include full width half distance calculation method, average angle full distance calculation method and minimum curvature method [4].During the operation, the east coordinate of the geographical drilling coordinates corresponds to the x position of Descartes, the north coordinate corresponds to the y position, the elevation corresponds to the Z position. The coordinates of the orifice x0、y0、z0 are known values.

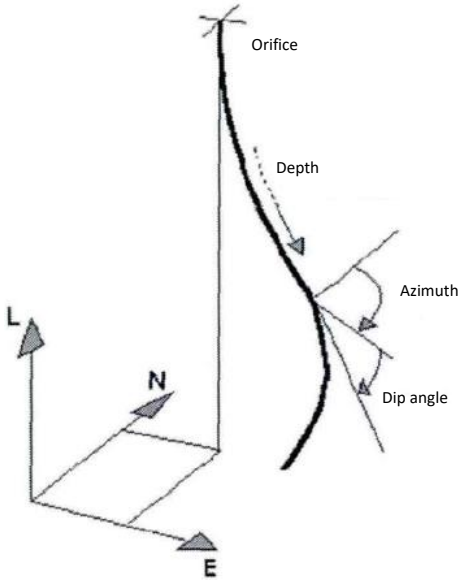

Figure 1. Borehole trajectory

1) Average angle full distance method

In the method, the drilling trace curve between the upper measuring point and lower measuring point is seen as a straight line. The average angle between the azimuth angle and inclination angle is taken as angle reference, and trace distance is taken as the length parameter, then conduct operation. The calculating formula of the space coordinate of the measuring point is as follows:

$$\begin{cases} x_i = x_{i-1} + L_i \cdot \sin\dfrac{\alpha_i + \alpha_{i-1}}{2} \cdot \cos\dfrac{\beta_i + \beta_{i-1}}{2} \\ y_i = y_{i-1} + L_i \cdot \cos\dfrac{\alpha_i + \alpha_{i-1}}{2} \cdot \cos\dfrac{\beta_i + \beta_{i-1}}{2} \\ z_i = z_{i-1} + L_i \sin\dfrac{\beta_i + \beta_{i-1}}{2} \end{cases} \quad (1)$$

2) Full angle half distance method

Take the half value of the measurement distance near upper measurement point, together with the half value corresponding to the lower measurement point, and the drilling trace curve is seen as a straight line. The length parameter is replaced with the half value of measurement distance, the angle reference uses hole inclined value of the upper and lower measurent points as the standard. Specific operations are as followed:

$$\begin{cases} x_i = x_{i-1} + \dfrac{L_i}{2}(\sin\alpha_{i-1}\cdot\cos\beta_{i-1} + \sin\alpha_i\cdot\cos\beta_i) \\ y_i = y_{i-1} + \dfrac{L_i}{2}(\cos\alpha_{i-1}\cdot\cos\beta_{i-1} + \cos\alpha_i\cdot\cos\beta_i) \\ z_i = z_{i-1} + \dfrac{L_i}{2}(\sin\beta_{i-1} + \sin\beta_i) \end{cases} \tag{2}$$

3) Minimum curvature method

Between the upper and lower measurent points is seen as arc section. Then the curvature value is minimum. The arc section and the drilling trace of the two monitoring points is tangent. The space coordinates operation of the measuring points are as follows:

$$\begin{cases} x_i = x_{i-1} + \dfrac{L_i Ks}{2}(\sin\alpha_{i-1}\cdot\cos\beta_{i-1} + \sin\alpha_i\cdot\cos\beta_i) \\ y_i = y_{i-1} + \dfrac{L_i Ks}{2}(\cos\alpha_{i-1}\cdot\cos\beta_{i-1} + \cos\alpha_i\cdot\cos\beta_i) \\ z_i = z_{i-1} + \dfrac{L_i Ks}{2}(\sin\beta_{i-1} + \sin\beta_i) \end{cases} \tag{3}$$

In the fomula, KS represents the correction coefficient or the circle coefficient.

$$Ks = \frac{\tan\dfrac{\gamma}{2}}{\gamma} \tag{4}$$

Wherein γ is the full bending angle

$$\gamma = a\cos(\cos\beta_{i-1}\cdot\cos\beta_i + \sin\beta_{i-1}\cdot\sin\beta_i\cdot\cos(\alpha_{i-1}-\alpha_i)) \quad (5)$$

2.2 Data structure of borehole 3D model

The numerical value of three dimensional visualization could be stored by the combination of numerical value table and geometric figures. Numerical tables store property values of the geometric patterns, and the geometric figures store the space area of the hole end and the model section. The value tables and pattern properties are in one-to-one correspondence, as shown in figure 2. Extract a numerical value from the value table and the corresponding pattern property could be obtained.

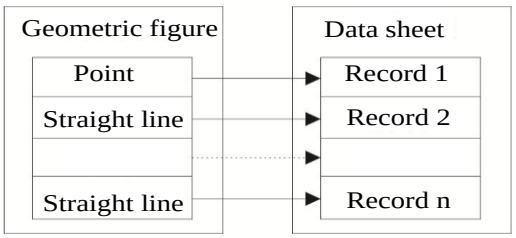

Figure 2. Data structure of borehole 3D model

2.3 3D model creation of drilling and attribute visualization

In the drilling 3D modeling, each drill is generated by one point, a series of continuous line segments and the corresponding numerical table record. The starting point coordinates and end point coordinates of sample section could be directly obtained accoring to located area of depths of the two points and drilling space trail curve. Add the corresponding attribute value of model section into numerical table.

The application of visualization could realize the presentation of different numerical information with color, pattern and different patterns context. For example, numerical value of drilling could be shown with a variety of colors of sample section; or present the grade value with curves at one end of the drilling hole.; we could use the the difference of context patterns to present lithology at one end of drilling hole. In addition, all the attribute values could be shown by words around geometric patterns. Figure 3 shows the histogram indicating the trace curve of drilling modeling space of one mine and the grade value of element Cu at the drilling hole.

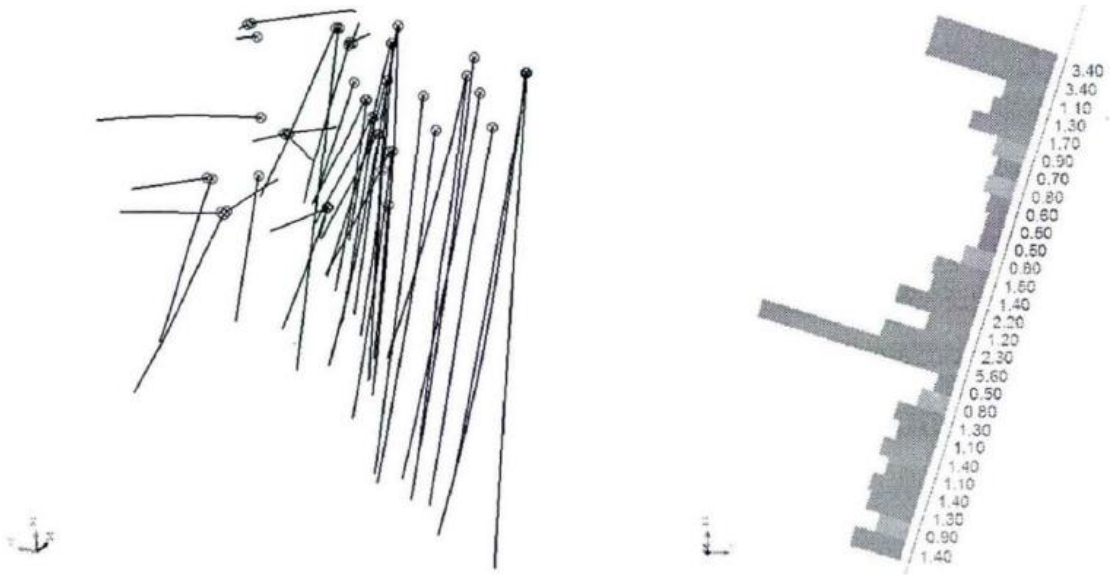

Figure 3. Presentation of borehole 3D modeling and visualization of properties

3. Surface model optimization algorithm based on outline

Contour overlay is to use a polygon or triangle to fill the adjacent external lines, forming the appearance of the object. Because the triangular grid is convenient and simple, and has a great use performance and a strong practicality. It is used and studied more widely [5]. In order to generate appearance of object, use triangular tiling to connect the external lines of the grid formed by adjacent triangles. And the pole is the point of the external lines. The way of the external line veneers includes: veneers based on the directed loop diagram and veneers based on apprearance adjustment. Each have its own advantages and disadvantages, and the application situation is totally different [6]. In terms of mine, the status of mineral aggregate changes all the time, while the length of the detection line section is affected by many kinds of factors and the distance is far, so the change of size and shape of the external line would happen at a high rate. In the paper. The multi-resolution veneer method with external lines to realize overall improvement is used and it could not only improve operation speed, but also be applied to the complex external lines.

$P_0, P_1, ..., P_{m-1}$ and $Q_0, Q_1, ..., Q_{m-1}$ are taken as sequence points on the corresponding external lines on the adjacent cross sections, external line section, namely the connection of adjacent sides on the same external lines P_iP_{i+1} or Q_iQ_{i+1}.

The span length is the side connected by two points on different external lines $\overline{P_iQ_i}$. The

basic triangle dough sheet refers to the dough sheet formed by the two span lengths generated by external line sections and the points on their both sides and the corresponding points on external line sections. Its characteristics are as follows[7]:

1) The pole of triangle dough sheet should include at least one Q;

2) One external line segment must and could only belong to one dough sheet;

3) Intersection between triangle dough sheets is not allowed;

4) Span length $\overline{P_iQ_i}$ exists only between two adjacent riangle dough sheets.

The shape and appearance that could be adopted must be in line with the above characteristics, but there are a lot of the adopted shape and appearance that are retained, corresponding to the external line. A lot of researches conduct analysis of the best way of the apprearance that could be adopted. Keppel[8] convert the veneer process between two external lines into the problem that could be discussed with diagram. Define the directed graph $G-\langle V,A\rangle$. Among it, the arc set A and all possible basic triangle dough sheet correspond to each other. The points $P_0,P_1,...,P_{m-1}$ and $Q_0,Q_1,...,Q_{n-1}$ correspond to pole set and gather all the possible span lengths together. A curve in the figure takes left span length of triangular face as the starting point, and the right span length as the end point[9]. Therefore:

$$V=\left\{v_{ij}\,\middle|\,i=0,1,...,m-1;\ j=0,1,...,n-1\right\} \tag{6}$$

Wherein v_{ij} corresponds to span length $\overline{P_iQ_i}$, so:

$$A=\left\{\langle v_{kl},v_{sl}\rangle\,\middle|\,s=k,t=l+_n1,s=k+_m1,t=1\right\} \tag{7}$$

So left span length $\overline{P_kQ_l}$ and $\langle V_{kl},V_{sl}\rangle$ correspond to each other and right spanlength is basic triangular dough sheet. In reality, the G represents a directed loop overing the torus,as shown in Figure 4 . The vertice v_{ij} are in row i, column j; the arc $\langle V_{ij},V_{i,j+_n1}\rangle$ is the horizontal curve between column j and column $i,j+_n1$, and the arc $\langle V_{ij},V_{i+_m1,j}\rangle$ is the vertical curve

between line i and line $i +_m 1$.

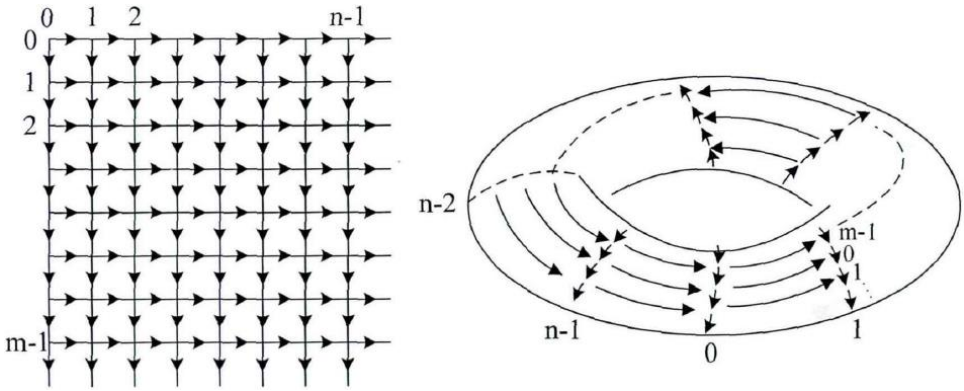

Figure 4. Loop diagram

The points gathering all the triangle dough sheet could be seen as a subordinate graphics of G, and one single acceptable subgraph S corresponds to one single acceptable appearance, as shown in figure 5. By this time, veneer between external lines has become the exploration of channels with the best advantage in the loop pattern. Each added curve represents one weight, then the measurement of triangle dough sheet presented by curves, the gross weight of all the curves corresponding to the acceptable appearance in directed loop graph is called value. When it comes to the peak, the best value is obtained.

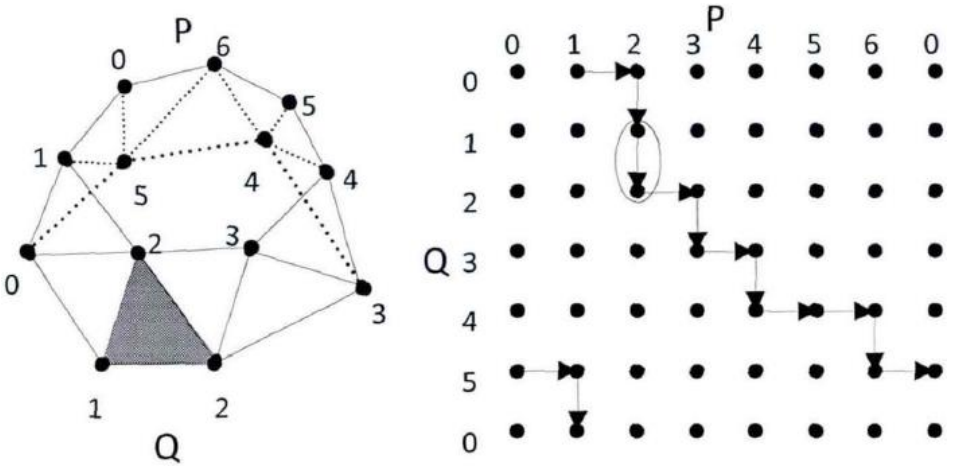

Figure 5. Directed loop graph of acceptable appearance

The reconstrucion of the appearance between two lines whose starting point and end point could not connect to form a loop is fundamentally the issue of external line veneer that is joined

the control requirements. The start point and the end point need to be connected to determine the span value $\overline{P_0Q_0}$ and $\overline{P_mQ_n}$, the veneer between two lines whose starting point and end point could not connect to form a loop is the exploration of the optimal path whose starting point (0,0) and end point (m-1,n-1) are fixed, as shown in figure 6.

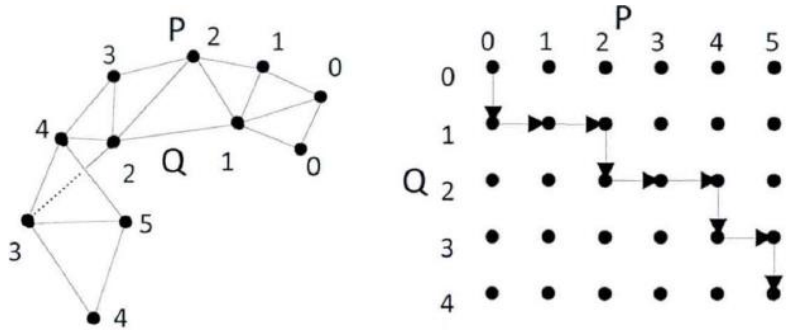

Figure 6. Optimal path with starting point and end point fixed

The exploration of the optimal path in plane figure G' could be seen as same operation in loop diagram G. Figure G' is produced by the combination of the two figure G, as shown in figure 7.

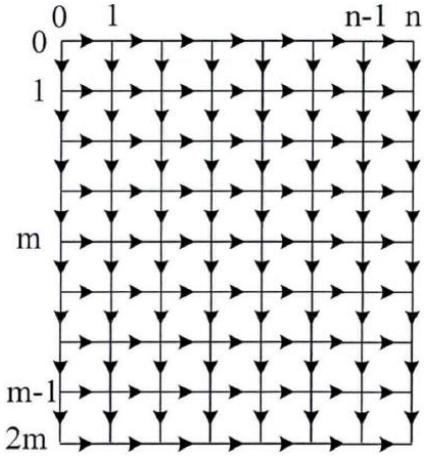

Figure 7. Figure G' formed by figure G

The path from starting point v_{i0} to end point v_{i0} in figure G corresponds to the path from starting point v_{i0} to end point $v_{m+i,n}$ in figure G'. So the best path could be obtained from all the paths from starting point v_{i0} to end point $v_{m+i,n}$ in figure G'. Assume that $p[i], i = 0,1,...,m-1$ is the best path from v_{i0} to $v_{m+i,n}$. In order to make the surface area of the lowest value, the shortest distance is considered as the best path. The key to find the path corresponding to the acceptable

appearance is to find out $p[0], p[1], ..., p[m-1]$ and select the shortest distance from them. Define G'(I,j) as subgraph of figure G.

The iterative algorithm for all path searching is as follows:

1) Execute for the first time to find P[0] and P[m], and P[m] is the shortest path from $v_{m,0}$ to $v_{2m,n}$.

2) Execute for the σth time, $\sigma=2,3,\ldots\lceil \log_2 m \rceil$ and a total of $2^{\sigma-2}$ paths are found out.

$p[\lfloor (2k-1)m/2^{\sigma-1} \rfloor]$ belongs to the subgraph

$G'(\lfloor (2k-2)m/2^{\sigma-1} \rfloor, \lfloor 2km/2^{\sigma-1} \rfloor), k=1,2,...,2^{\sigma-2}$

3) Execute for the last time, namely the $\lceil \log_2 m \rceil+1$th,

$G'(\lfloor (2k-2)m/2^{\lceil \log_2 m \rceil} \rfloor, \lfloor 2km/2^{\lceil \log_2 m \rceil} \rfloor)$, each path $p[\lfloor (2k-1)m/2^{\lceil \log_2 m \rceil-1} \rfloor]$ is found out,

$k=1,2,...,2^{\lceil \log_2 m \rceil-1}$.

Compared with a total of m path operations, the execution frequency of the iterative algorithm is $\lceil \log_2 m \rceil+1$ and has been greatly improved.

The shortest distance from one single starting point in the graph to the other points could be found out using the Decoster algorithm (Dijkstra). The basic principle is that accuracy of the operation method could be ensured by adding a new point with the shortest interval one time and at the same time changing interval of the near points, because there will be no points with smaller intervals than this point, so the interval of this point is fixed. Assume that starting point of the path is vs and the distance dist[v] of point v is the interval from the starting point to v. The algorithm flow is [10]:

1)Initialize the distances of all points. The source point vs is set as o, and the other points are set as infinity.

2) Make a mark on all the points that have not been visited, and take vs as the current point.

3) For the current point, analyze and calculate the distances of these points, and find out the points with minimum interval and note down.

4) Mark the state of the current point visited.

5) If all points have been visited, the algorithm ends. Otherwise, set up minimum distance, the next point to visit is the continuation of the current point.

4. Application of mineral deposit modeling technology in mine

4.1 Drilling data management and visualization

According to the numerical drilling table set above, clear and integrate the initial geological value, and reserve and store the big hole, measurement slope, sample plate and lithologic data table. All the original geological values are drilling data including drilling value and numerical exploration drilling value. Conduct the reconstruction of the drilling hole, measurement inclination and sample value used in the establishment of mineral resource model according to the corresponding table and store them into the system for further use.

Table 1. Data table of drilling hole

Drilling name	east coordinate	north coordinate	heigth	hole depth	exploration line number
B4CK1	6623.1	3572.5	533.3	71.14	4
B6CK1	6649	3529.1	533.05	66.09	6
B10CK1	6757.7	3472.25	532.75	31.55	10
B12CK1	6779.2	3427.6	532.7	45.34	12
B14CK1	6747.2	3353.9	532.45	70.92	14
B16CK1	6764.4	3306.4	532.5	55.27	16
B18CK1	6649.75	3182	531.27	89.89	18
ZK32-32	7005.284	3006.630	659.958	42.37	32
ZK32-33	7049.771	3032.777	659.578	57.34	32
ZK34-29	7031.801	2963.547	659.111	60.88	34
ZK34-30	7032.126	2963.504	666.301	43.31	34
ZK34-31	7032.646	2966.806	660.381	71.86	34
ZK38-27	7082.786	2879.476	659.285	59.82	38
ZK38-28	7084.693	2881.611	660.355	60.77	38
ZK42-24	7098.021	2772.040	660.663	37.91	42

ZK42-25	7149.996	2802.287	660.845	50.68	42
ZK42-26	7151.387	2804.477	660.945	79.68	42
ZK44-21	7150.130	2743.077	659.565	70.37	44
ZK44-22	7150.823	2743.477	661.065	47.60	44
……	……	……	……	……	……

Among them there are totally 586 records including 39 drilling holes, 119 geological surface drilling, 157 holes drilled along the direction of the detection line, 262 holes drilled along the horizontal detection, 9 holes of other types. Part of the table is shown in table 1.

After inputting the drilling value, we could conduct various operations to the numerical table in the system including delete, modify and add numerical value. The accuracy of the initial numerical value determines correction rate and error number of the numerical value. If the number of errors is large, there will be much trouble to correct one by one according to the error mark. So, the system will mark the numerical sheet in which error occurs and the corresponding mark in the error report. So, the error mark would be found out in the numerical table just by double-click on the error mark with the mouse.

4.2 Fault shown model

The studied deposit is a very complex collection and is divided into numerous small orebodies by mine fault layers. The structure of fault layers is very complex. Therefore, in terms of these deposit modeling and numerical information appears to have profound and practical significance to research and exploration. It is of great and practical significance to present these numerical values and information for research and exploration. Before creating model, first gather all the detection line section figures and central paragraph geological fiugres containing fault layer line for integration and exploration, then input the information data on map into DIMINE system and construct the model with the improved operation method of external line veneer.

A total of 40 fault layers exist in the mining area and divide it into three parts according to the location so that it could be very easy to see the direction of the fault layers in the established

model, and further more easy to be rebuilt and identified. The ordered fault layer lines are shown in figure 8.

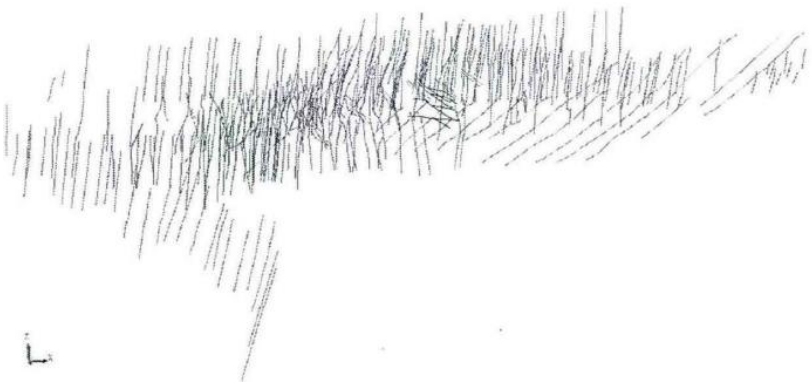

Figure 8. Well ordered fault layer lines

After the integration of the fault layer lines is completed, we could establish models of each fault layer according to their direction as shown in Figure 9.

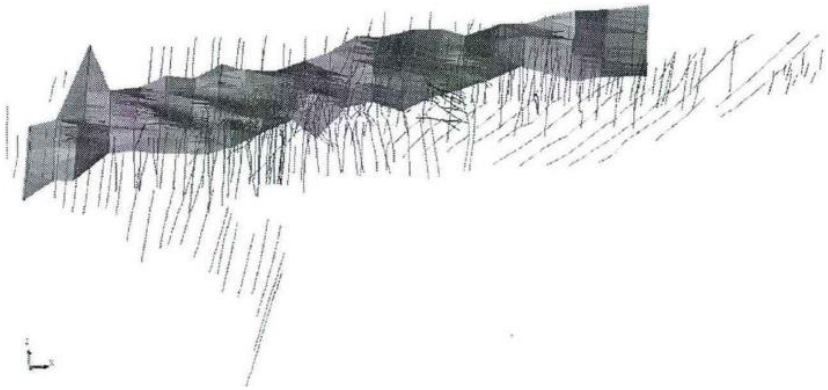

Figure 9. Establishment of surface model of fault layer

When calculating the surface model, information data of all the fault layers are needed. So the establish quality of fault layer model has a direct impact on the following research work. In addition, the ore body will be divided by the fault layers so the correspondance of the ore body and the segmentation of the fault layers must be ensured. The established surface model of fault layer is shown in Figure 10.

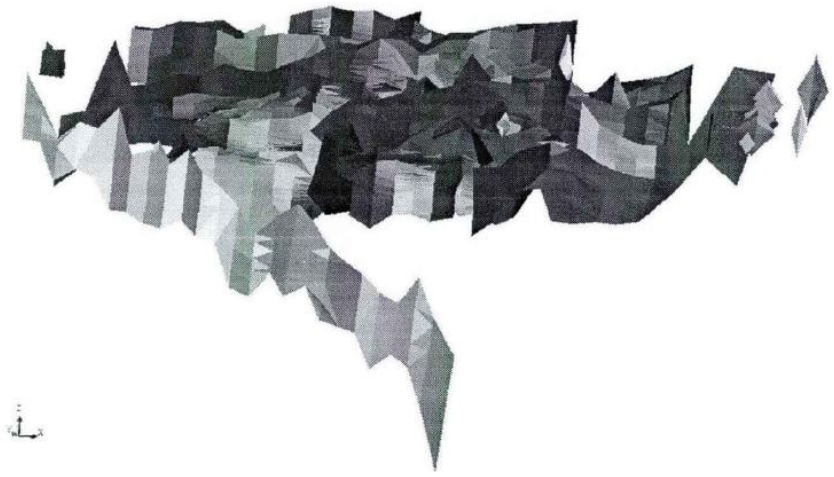

Figure 10. Surface model of fault layer

4.3 Surface model of ore body

Creating the model of surface model of mineral geological body is very important to the creation of the set model of the whole mineral geological body. The surface model of fault layers created previously mainly presents the relationship of the mineral geological body segmentation. The surface model of the mineral geological body is also the foundation of the creation of discrete model. The creation of surface model of the mineral geological body is through the external lines of mineral geological bodies at all sections and consistent with the fault lines, and to clear and integrate the external lines of mineral geological body at all sections, then input it into the software system of DIME and conduct modification according to the grade presentation situation of drilling 3D model. The external lines of the revised mineral geological body are shown in Figure 11, which is the external lines of the mineral geological body I2. And figure 12 the external lines of all the 7 mineral geological bodies.

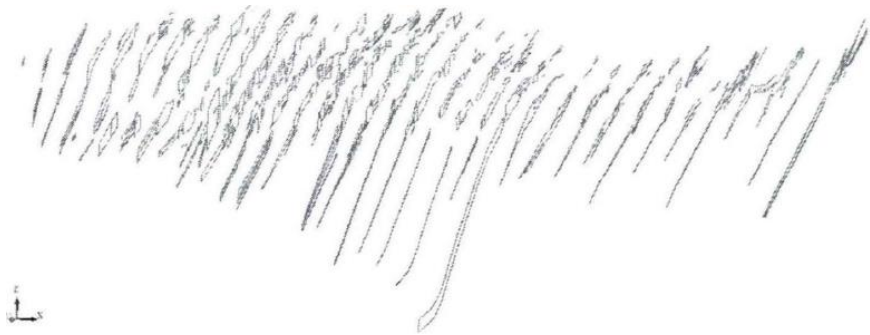

Figure 11. Eternal lines of I2 mineral bodies

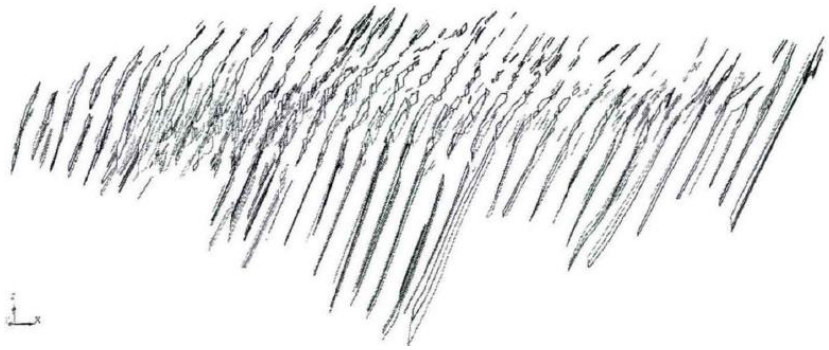

Figure 12. Eternal lines of all the 7 mineral bodies

The surface models are respectively established for the outlines of each ore body, as shown in figure 13.

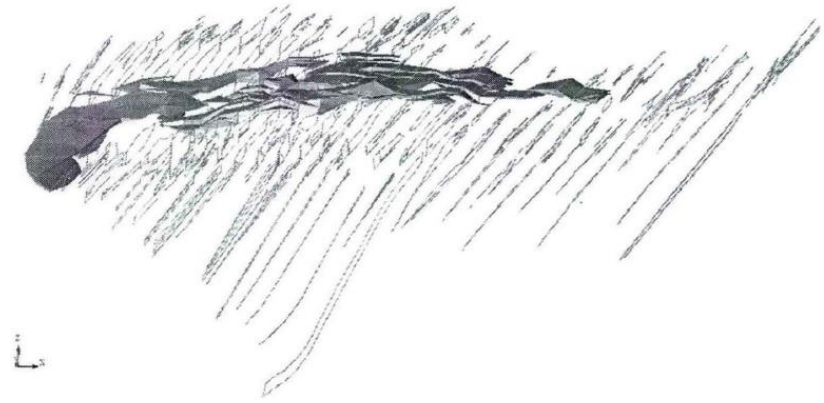

Figure 13. Establishment of surface model of I2 ore body

From the surface of external lines, it could be seen that there is a straight line to connect the two points near the external lines of the sections. But in reality, the fault layer face is likely to be a space curved surface and the situation in which fault layer does not correspond to mineral geological body might also occur, including that mineral geological bodies has exceeded the fault layer and that there are gaps between the fault layer and mineral geological bodies. In order to make the fault layer model and surface model of mineral geological bady completely corresponding to each other, it needs to calculate the surface model of fault layer and the surface model of mineral geological body and remove the excess part of mineral geological body with fault layer and extend the mineral geological body that has gaps with fault layer over fault layer and remove the redundant part with fault layer, through these methods to ensure the correspondance between fault layers and mineral geological bodies.

Figure 14 shows a small part of fault layer and mineral geological body. In the figure, the latter is divided into two parts, and one has gaps with fault layer, the other is over fault layer. In the situation, it is necessary to appropriately increase the distance of the two parts of mineral geological body and make them extend fault layer as shown in figure 15. Next remove the reduntant part through calculation to make fault layer correspond to mineral geological body totally, as shown in figure 16.

Figure 14. Position relationship between ore body and fault layer

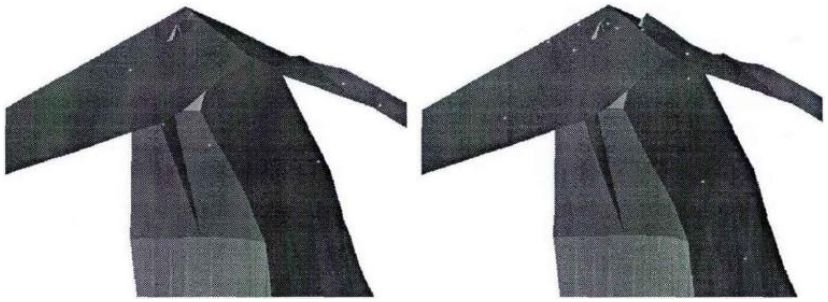

Figure 15. position relationship betweem fault layer and ore body after the parts are extended

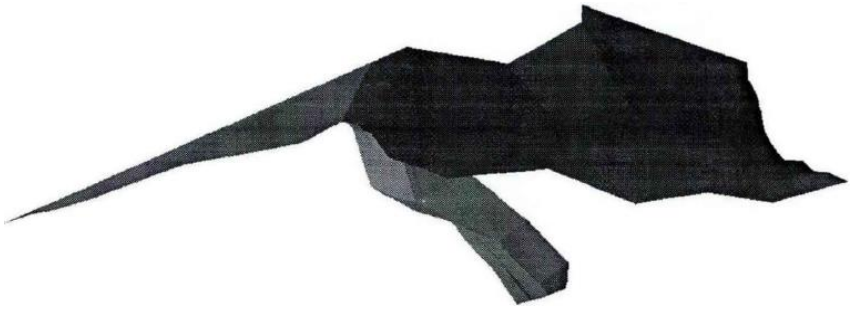

Figure 16. Fault layer and ore body totally corresponding to each other after calculation

In the creation process of mineral geological body model, when the surface reconstruction of the two external lines at the section whose distance is small and the corresponding external lines

at the near section is conducted respectively, the two models might produce intersec. In order to really present the space relationship of mineral geological bodies, during the model establishment, it needs to calculate the two mineral geological bodies that have intersections and remove the redundant part to make them totally corresponding to each other. The calculation method is the same with that of fault layer and mineral geological body and the difference is the calculation between mineral geological bodies would be conducted only when the intersection occurs.

5. Conclusion

As the foundation and focus of the digital mine software system, the 3D geological modeling of mineral aggregate plays an important role in the development and the KUAN management of mine resources and the information process of the mining industry. This paper briefly discusses the improved calculation method of appearance veneer, and researches the multi-resolution veneer operation method aiming at the disadvantage of the improved calculation method of external lines veneer in the timeliness. Use the improved calculation method of external lines veneer to the external lines with low resolution and add the vertexes to current tables one by one in order to obtain a new appearance. Taking the copper deposit as an example, the block model, surface model of fault layer and surface model of mineral aggregate are created precisely to connect the geological body as well as the project model and tetrahedral mesh model, so the obtained operation model could calculate precisely the project mining value under complex geological environment.

References

1. Kyle J R, Ketcham R A. Application of high resolution X-ray computed tomography to mineral deposit origin, evaluation, and processing. Ore Geology Reviews, 2015, vol. 65, pp. 821-839.
2. Alaei M S, Karimi M, Mesgari M S, et al. Modeling process of mineral potential mapping using fuzzy inference systems (case study: chah firoozeh copper deposit). 2014.
3. Tehrani M A M, Asghari O, Emery X. Simulation of mineral grades and classification of mineral resources by using hard and soft conditioning data: application to Sungun porphyry copper deposit. Arabian Journal of Geosciences, 2015, vol. 6, no. 10, pp. 3773-3781.

4. Jing Y, Liu X, Bi L. Key techniques for 3D visual modeling of complex mineral deposits. Zhongnan Daxue Xuebao, 2014, vol. 45, no. 9, pp. 3104-3110.
5. Han Q, Gong X, Tian H. Application of IP to exploration in Sujiquandong gold deposit. Contributions to Geology & Mineral Resources Research, 2016.
6. Sun Y, Ma S A, Huang L, et al. Sandaozhuang Open-Pit Quality Block Modeling Based on Engineering Geological Profile. Advanced Materials Research, 2014, 962-965, pp. 959-963.
7. Miao J X, Li C X, Qu J, et al. 3D Geological Modeling (Deposit Scale) for Granite Rock-Mass in Yuku Area, Luanchuan, China. Advanced Materials Research, 2014, 962-965, pp. 92-98.
8. Perevertailo T, Nedolivko N, Prisyazhnyuk O, et al. Application of geologic-mathematical 3D modeling for complex structure deposits by the example of Lower- Cretaceous period depositions in Western Ust - Balykh oil field (Khanty-Mansiysk Autonomous District)[C]// 2015, pp. 012016.
9. H U, Han X, Yusheng L I, et al. Application of GIS Technology for Mineral Exploration Prediction: Taking Qinghai Kekexili Gaodi Sheet as an Example. Acta Geologica Sinica, 2014, vol. 88, no. s2, pp. 1246-1246.
10. Boutroy E, Dare S A S, Beaudoin G, et al. Magnetite composition in Ni-Cu-PGE deposits worldwide: application to mineral exploration. Journal of Geochemical Exploration, 2014, vol. 145, pp. 64-81.